Amino Acids (2007) 32: 347–357
DOI 10.1007/s00726-007-0493-4
Printed in The Netherlands

Amino Acids

Mass spectrometric analysis of protein histidine phosphorylation

X.-L. Zu[1], **P. G. Besant**[1], **A. Imhof**[2], and **P. V. Attwood**[1]

[1] School of Biomedical, Biomolecular and Chemical Sciences (M310), The University of Western Australia, Crawley, WA, Australia
[2] Department of Molecular Biology, Adolf-Butenandt Institute, Histone Modifications Group, Ludwig-Maximilians-University of Munich, Munich, Germany

Received November 1, 2006
Accepted January 10, 2007
Published online February 28, 2007;

Summary. Protein histidine phosphorylation is now recognized as an important form of post-translational modification. The acid-lability of phosphohistidine has meant that this phosphorylation has not been as well studied as serine/threonine or tyrosine phosphorylation. We show that phosphohistidine and phosphohistidine-containing phosphopeptides derived from proteolytic digestion of phosphohistone H4 are detectable by ESI-MS. We also demonstrate reverse-phase HPLC separation of these phosphopeptides and their detection by MALDI-TOF-MS.

Keywords: Phosphohistidine – Mass spectrometry – Phosphoamino acid analysis – Histone H4 – Phosphopeptide – Histidine kinase

Introduction

Protein phosphorylation is probably the most important post-translational modification in terms of its roles in the regulation of cellular function. To date, there has been most interest in the actions of serine/threonine and tyrosine kinases and their phosphorylated products. Most methodologies having been designed to investigate this type of protein phosphorylation and in recent years these have included the development of a number of mass spectrometric approaches.

Another form of protein phosphorylation is catalysed by histidine kinases, which play important roles in signal transduction in prokaryotes and lower eukaryotes. In these organisms they are known as two-component histidine kinases (Stock et al., 2000). The first component is usually a membrane-bound receptor-like protein, which has a cytoplasmic histidine kinase domain, which is activated after stimulation and subsequent dimerisation of the receptor. The histidine kinase domains then cross phosphorylate a highly conserved histidine residue on the other member of the dimer. The second component of the system is a response regulator protein, which is often a transcription factor, the phosphoryl group from the phosphohistidine of the first component is transferred to a conserved aspartate residue on the response regulator protein, thus activating it (Stock et al., 2000). There are more complex signalling systems, e.g. the osmosensing Sln1p system in yeast, where initial phosphotransfer occurs to an aspartate on another domain of the histidine kinase, this then transfers its phosphoryl group to a histidine on a phosphorelay protein prior to the ultimate phosphoryl transfer to aspartate on the response regulator protein.

An increasing number of histidine kinase activities have also been described in mammalian cells (Besant et al., 2003; Besant and Attwood, 2005). For example, NDP kinase was regarded as a housekeeping enzyme which maintained cellular levels of nucleoside di- and tri-phosphates by catalysing their interconversion via an active site phosphohistidine intermediate phospho-transfer mechanism (Munoz-Dorado et al., 1993). NDP kinase has been reported to be a protein histidine kinase that plays roles in cellular signalling by phosphorylating annexin I (Treharne et al., 1994, 2001; Muimo et al., 1998, 2000) and the β-subunits of trimeric G-proteins (Uesaka et al., 1987; Kimura and Shimada, 1988; Kikkawa et al., 1990; Cuello et al., 2003; Hippe et al., 2003).

The existence of histone H4 histidine kinases (HHKs) has been well documented from studies in yeast (Huang et al., 1991), porcine thymus (Besant and Attwood, 2000), rat liver (Smith et al., 1973; Chen et al., 1974, 1977; Tan et al., 2004) and human liver (Tan et al., 2004). There is some evidence from a study on human liver

1 SGRGKGGKG LGKGGAKRHR KVLRDNIQGI TKPAIRRLAR RGGVKRISGL 50
51 IYEETRGVLK VFLENVIRDA VTYTEHAKRK TVTAMDVVYA LKRQGRTLYG FGG 102

Fig. 1. Amino acid sequence of histone H4. S is replaced by T in drosophila histone H4. The preparations of recombinant drosophila histone H4 contained a mixture of protein with the amino acid sequence indicated above and protein with the N-terminal methionine in place. For this reason, the numbering system adopted for the drosophila sequence is 1–103, whilst that for the bovine histone H4 is 1–102

and hepatocellular carcinoma, that the HHK may be an oncodevelopmental marker (Tan et al., 2004).

Phosphohistidine differs from phosphoserine, phosphothreonine and phosphotyrosine in that it is acid-labile while the phosphoester phosphoamino acids are acid-stable. Since many of the techniques used to study protein phosphorylation involve acidic treatments, evidence of histidine phosphorylation is often lost. In recent years, our laboratory and others have been involved in developing methods to analyse and measure protein histidine phosphorylation and histidine kinase activity (Wei and Matthews, 1990, 1991; Medzihradszky et al., 1997; Besant et al., 2000; Napper et al., 2003; Tan et al., 2003; Wind et al., 2005). There have been few reports of the use of mass spectrometry (MS) to detect phosphohistidine and analyse proteins and peptides containing phosphohistidine. Medzihradszky et al. (1997) analysed a synthetic phosphopeptide by matrix-assisted laser desorption ionisation (MALDI)-high-energy collision-induced dissociation (CID) MS. Wind et al. (2005) investigated phosphorylated CheA-H, the histidine-containing domain of the two component histidine kinase, CheA, by ^{31}P element-MS and electrospray ionisation (ESI)-MS. These authors could not detect phosphopeptides in a tryptic digest of phospho-CheA-H, so had to analyse the intact phosphoprotein and could not then specifically identify the site of phosphorylation. Napper et al. (2003) analysed partial tryptic digests of phospho-HPr by MALDI-time of flight (TOF)-MS following phosphopeptide enrichment using immobilized Cu(II) ion affinity chromatography.

In the current work, we performed a much more comprehensive MS analysis of a phosphohistidine-containing phosphoprotein. We chose histone H4, phosphorylated specifically on its histidine residues by treatment with phosphoamidate as the model system. Histone H4 was chosen because it is a substrate of HHK, which appears to have interesting biological significance (see above) and because it possesses only two histidine residues, H18 and H75 (see Fig. 1), both of which have been identified to be phosphorylated by HHK (Fujitaki et al., 1981). We have performed phosphoamino acid analysis using ESI-MS/MS and analysis of the phosphopeptides using both MALDI-TOF-MS and ESI-MS/MS on proteolytic digests of phosphohistone H4.

Materials and methods

Materials

Bovine histone H4 was purified from Type-IIS histone (Sigma-Aldrich, Australia) as described previously (Tan et al., 2004). Recombinant drosphilia histone H4 was expressed in *E. coli* as described by Bonaldi et al. (2004). Potassium phosphoamidate was synthesised and purified as described by Wei and Matthews (1991). Trypsin and pronase E (*Streptomyces griseus*) were obtained from Sigma-Aldrich, Australia, while endoproteinase Asp-N was purchased from Roche Diagnostics, Germany.

Mass spectrometers

ESI-MS and ESI-MS/MS was performed, on an Applied Biosystems QSTAR pulsar *i* quadrupole time-of-flight instrument. The QSTAR pulsar *i* was equipped with a turbospray ion source through which samples were infused at flow rates of either indicated. The QSTAR was calibrated in positive ion mode using the MS/PS product ions (b_2 and y_{11}) of [Glu1]-fibrinopeptide B (EGVNDNEEGFFSAR) and in the negative ion mode with taurocholic acid and the SO_3^- fragment ion. MALDI-TOF-MS was performed on an Applied Biosystems Voyager DE STR mass spectrometer.

Phosphorylation of histone H4

Bovine histone H4 (5 mg ml^{-1}) was incubated for 3 h at room temperature with 100 mg potassium phosphoamidate in 1 ml water, with the pH adjusted to 8.0 with KOH. The reaction mixture was dialysed against 20 mM ammonium bicarbonate (2 l) at 4 °C for 5 h prior to immediate proteolytic hydrolysis. Recombinant Drosphila histone H4 (1 mg ml^{-1}) was incubated overnight, at room temperature, with 25 mg potassium phosphoamidate in 1 ml water, with the pH adjusted to 7.2 with KOH. The reaction mixture was lyophilised, resuspended in 100 µl 10 mM ammonium bicarbonate and stored at −20 °C, where it was found to be stable for up to 3 months.

Proteolytic digestion of phosphohistone H4

The dialysed solution of bovine phosphohistone H4 (4 mg ml^{-1}) in 20 mM ammonium bicarbonate was incubated overnight at room temperature with either pronase E (500 µg ml^{-1}) or trypsin (50 µg ml^{-1}). Approximately, 0.1–0.2 mg of recombinant *Drosphila* phosphohistone H4 were incubated with 1–2 µg of endoproteinase Asp-N at 37 °C in 40 µl 10 mM ammonium bicarbonate. Reaction mixtures were concentrated about 5-fold by lyophilisation and stored at −20 °C until required. The H4 molecule was expressed in *E. coli* and purified as described previously (Bonaldi et al., 2004) leading to a mixture of H4 molecules in which the N-terminal methionine had been cleaved in approximately 50% of all H4s. This results in the generation of two types of N-terminal AspN fragments, which we termed 1-24 and 2-24 depending on whether the methionine is present or not.

ESI-MS analysis of proteolytic digests of bovine phosphohistone H4

For negative ion MS, the tryptic or pronase E digests were diluted 1:10 with a 4.5% ammonia solution in 70% methanol. For positive ion MS, the

tryptic or pronase E digests were diluted 1:2 with 10 mM ammonium bicarbonate in a 75% solution of methanol. The samples were sprayed directly into the Applied Biosystems QSTAR pulsar *i* electrospray ionisation time-of-flight mass spectrometer.

MALDI-TOF-MS analysis of proteolytic digests of recombinant drosophila histone H4 and phosphohistone H4

The digest samples were desalted on C_{18}Zip Tips (Millipore, USA) by loading the digests, washing with water and eluting the digests directly on to the MALDI target plate with the 1–2 µl of matrix. Matrix was a saturated solution of α-cyano-4-hydroxycinammic acid in 50% acetonitrile containing either 0.1% trifluoroacetic acid (pH 2) or 10 mM ammonium bicarbonate (pH 8). Spectra were obtained by operating the Voyager DE STR instrument, as indicated, in either linear or reflector mode. The accelerating voltage was 20 kV, the grid was set to 94% (linear mode) or 66% (reflector mode) and at least 400 shots were taken to obtain each spectrum.

Reverse-phase HPLC separation of phosphopeptides in the endoproteinase Asp-N digest of drosophila phosphohistone H4

Approximately, 10 µg of the phosphohistone H4 digest was loaded on to a Gemini C_{18} reverse-phase column (Phenomenex, Germany: 50 × 3 mm; 5 µm) that had been equilibrated with 0.1% trifluoroacetic acid. The peptides and phosphopeptides were eluted by application of a linear gradient of 0–90% acetonitrile, 0.1–0.065% trifluoroacetic acid at a flow rate of 200 µl min^{-1}. The eluted peptides and phosphopeptides were detected using a U.V. absorbance detector set at a wavelength of 214 nm and 20 µl fractions were collected for analysis by MALDI-TOF-MS. As soon as possible after the elution of each peak, 10 µl of 10 mM ammonium bicarbonate was added to the corresponding fractions and samples were prepared for MALDI-TOF-MS by mixing with matrix solution and spotting on to the target plate.

Results and discussion

ESI-MS phosphoamino acid analysis of pronase E digest of phosphohistone H4

Figure 2a shows that a negative ion with an m/z of 234.1216 amu is a precursor of an ion with an m/z of −79 amu, which is the m/z of the PO_3^- ion. The theoretical monoisotopic m/z for the singly charged negative ion of phosphohistidine is 234.0285 amu. There were a number of other precursors detected in Fig. 2a, however none of these precursors has a mass corresponding to a negative ion of phosphoserine, phosphothreonine or phosphotyrosine (or indeed a negative ion of an amino acid). The identity of these precursor ions was not further investigated. Figure 2b shows the negative ion mass spectrum of the pronase E digest of phosphohistone H4 and indicated on the spectrum are signals with m/z values corresponding to singly charged, individual amino acid ions and some possible dipeptide ions. There is a large signal 234.1615 amu, however this appears to be part of an isotopic series of a singly charged ion with a monoisotopic

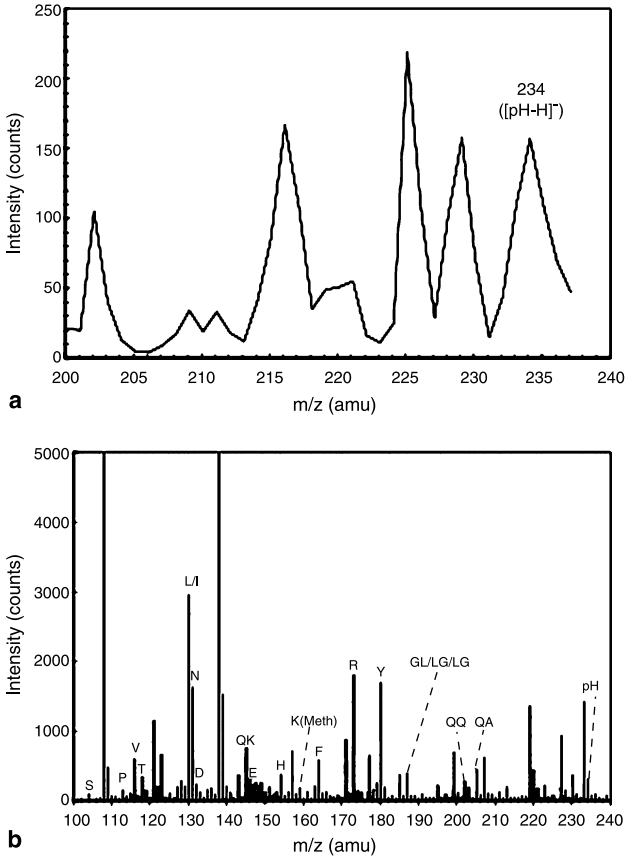

Fig. 2. Negative ion ESI-MS experiments on the pronase E digest of phosphohistone H4. The sample was infused at 5 µl min^{-1} using a declustering potential of −50 V. **a** Precursor ion spectrum detecting the precursors of the −79 amu ion (PO_3^-). 300 scans were accumulated with a collision energy of −50 V. **b** MS scan of the digest where 300 scans were accumulated

m/z of 233.1569 amu. There is, however, a much smaller shoulder peak at 234.0359 amu, which has no counterpart in the 233 amu region of the spectrum, that does closely correspond to the monoisotopic m/z of the singly charged phosphohistidine ion (234.0385 amu).

Figure 3a shows the positive ion mass spectrum of the pronase E digest of phosphohistone H4 and indicated on the spectrum are signals with m/z values corresponding to singly charged, individual amino acid ions and some possible dipeptide ions. A signal is indicated corresponding to a singly charged ion with a monoisotopic m/z of 236.0832 amu which closely corresponds to the theoretical monoisotopic m/z of the singly charged ion of phosphohistidine (236.0903 amu). Figure 3b shows the product ion spectrum derived from collision-induced dissociation of the ion with an m/z of 236 amu shown in Fig. 3a. Indicated on the spectrum are signals corresponding to expected product ions of phosphistidine. Strong

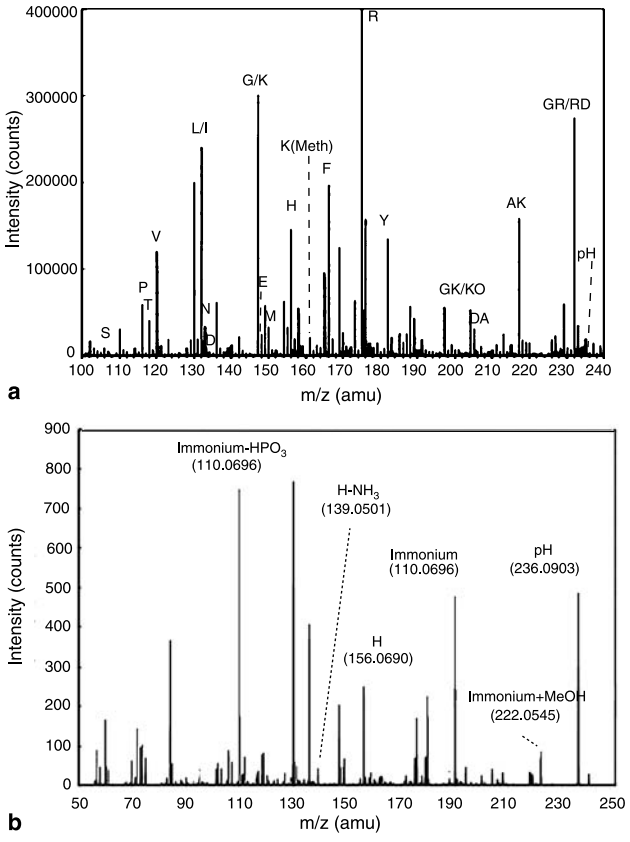

Fig. 3. Positive ion ESI-MS/MS spectrum showing product ions of phosphohistidine ($[M+H]^+$, $m/z = 236.0903$ amu) obtained from the pronase E digest of phosphorylated histone H4 that match that correspond to predicted product ions. A product ion spectrum was obtained where the sample was infused at flow rate of 1 µl min^{-1} with a declustering potential of 30 V and collision energy of 25 V. Where the observed signal was within 0.06 amu of the theoretical mass of a product ion and had a minimum peak height equal to 20 counts, the signal is labelled with its m/z value and the identity of the corresponding product ion

signals were observed that have m/z values that closely correspond to the theoretical m/z values of immonium ions of phosphohistidine (190.0376 amu) and histidine (110.0713 amu). In addition, a strong signal was observed corresponding to the histidine ion (156.0768 amu). Signals were also observed that could correspond to the methanol adduct of the immonium ion of phosphohistidine (222.0545 amu) and the deaminated phosphohistidine ion (139.0501).

We have thus obtained convincing evidence of histidine phosphorylation of histone H4, through the detection of a negative ion with an m/z that is close to that expected for the corresponding ion of phosphohistidine that produces a product ion matching the m/z of PO_3^-. In positive ion mode, an ion was detected with an m/z that is close to that expected for the corresponding ion of phosphohistidine that produces a number of product ions that are characteristic of phosphohistidine.

MALDI-TOF-MS analysis of endoproteinase Asp-N digests of histone H4 and phosphohistone H4

Figure 4a shows the linear MALDI-TOF spectrum of an endoproteinase Asp-N digest of unphosphorylated drosophila histone H4 in which the major peaks observed had m/z values corresponding to those expected peptide ions in this mass range (see Table 2). Figure 4b and c shows linear MALDI-TOF spectra of the endoproteinase Asp-N digest of phosphorylated drosophila histone H4 in either matrix at pH 2 or matrix at pH 8, respectively. Note that the closeness of the m/z values of the ions $[H4\ 86\text{-}103]^+$ and $[H4\ 69\text{-}85p]^+$ makes deconvolution of the signals difficult. The absolute signal intensities of corresponding ions are lower in (c) compared to (b). However, the estimated ratios of the signal intensities of the phosphopeptide ions ($[H4\ 1\text{-}24p]^+$ and $[H4\ 2\text{-}24p]^+$) to those of the corresponding unphosphorylated peptide ions ($[H4\ 1\text{-}24]^+$ and $[H4\ 2\text{-}24]^+$) are higher (23 and 11% higher) in (c) compared to (b), suggesting that there has been less dephosphorylation of phosphopeptides in the pH 8 matrix compared to the pH 2 matrix. This is not unexpected given the acid-lability of phosphohistidine and there is thus a trade of between the higher signal intensities in the low pH matrix, due to increased protonation of the peptides and the increased dephosphorylation of phopshohistidine under these conditions. Figure 4d is a reflector MALDI-TOF spectrum of the same sample used in Fig. 4c. The estimated ratios of the signal intensities of the phosphopeptide ions ($[H4\ 1\text{-}24p]^+$ and $[H4\ 2\text{-}24p]^+$) to those of the corresponding unphosphorylated peptide ions ($[H4\ 1\text{-}24]^+$ and $[H4\ 2\text{-}24]^+$) in Fig. 4c are 0.48 and 0.39, respectively, while the corresponding ratios in Fig. 4d are 0.10 and 0.17. This indicates that considerable post-source decay of the phosphopeptide ions is occurring, which is detected in the reflector MALDI-TOF MS spectrum. The most likely fragmentation process involves the neutral loss of HPO_3. In the reflector MALDI-TOF spectrum two additional peaks are apparent (i and ii) with m/z values of 2362.23 and 2493.13, which are not visible when the spectra are acquired in linear mode. These could, perhaps, be fragments of the $[H4\ 24\text{-}67]^+$ ion, however the fact that the mass difference between these ions and the two phosphopeptide ions, $[H4\ 2\text{-}24p]^+$ and $[H4\ 1\text{-}24p]^+$, respectively, is 92 amu in both cases is suggestive that they are metastable fragmentation products of these ions. However, we are not aware of any reports of such a mass loss

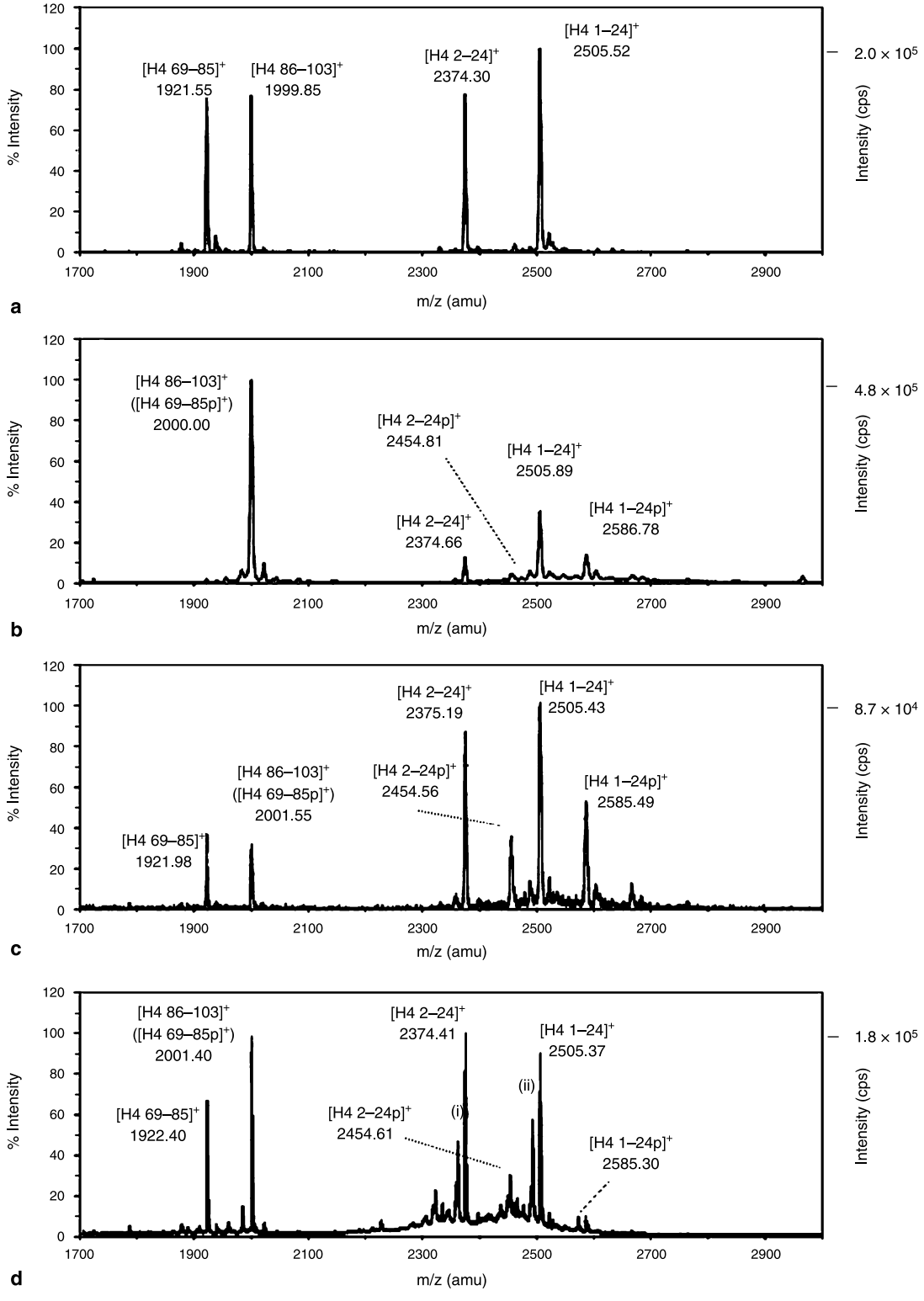

Fig. 4. Positive ion MALDI-TOF MS spectra of endoproteinase Asp-N digests of **a** histone H4, **b**–**d** phosphohistone H4. In **a**, **c** and **d** the matrix used to prepare the sample comprised α-cyano-4-hydroxycinnamic acid in 50% acetonitrile/10 mM ammonium bicarbonate, pH 8. In **b** the matrix was as above but with 0.1% trifluoroacetic acid replacing the ammonium bicarbonate and the pH of the matrix was 2. The spectra **a**–**c** were collected in linear mode, while spectrum **d** was collected in reflector mode. The signals that are close to the theoretical m/z values (see Table 2), of peptide and phosphopeptide ions derived from Asp-N digests of histone H4 and phosphohistone H4 are labelled with m/z values and the corresponding (phospho)peptide ion, where the numbers indicate the sequence positions in full length drosophila histone H4 of the N- and C-terminal peptide amino acids, p indicates a phosphopeptide. In **d** there are two unidentified major peaks in the spectrum labelled (i) and (ii), with m/z values of 2362.23 and 2493.13 amu, respectively

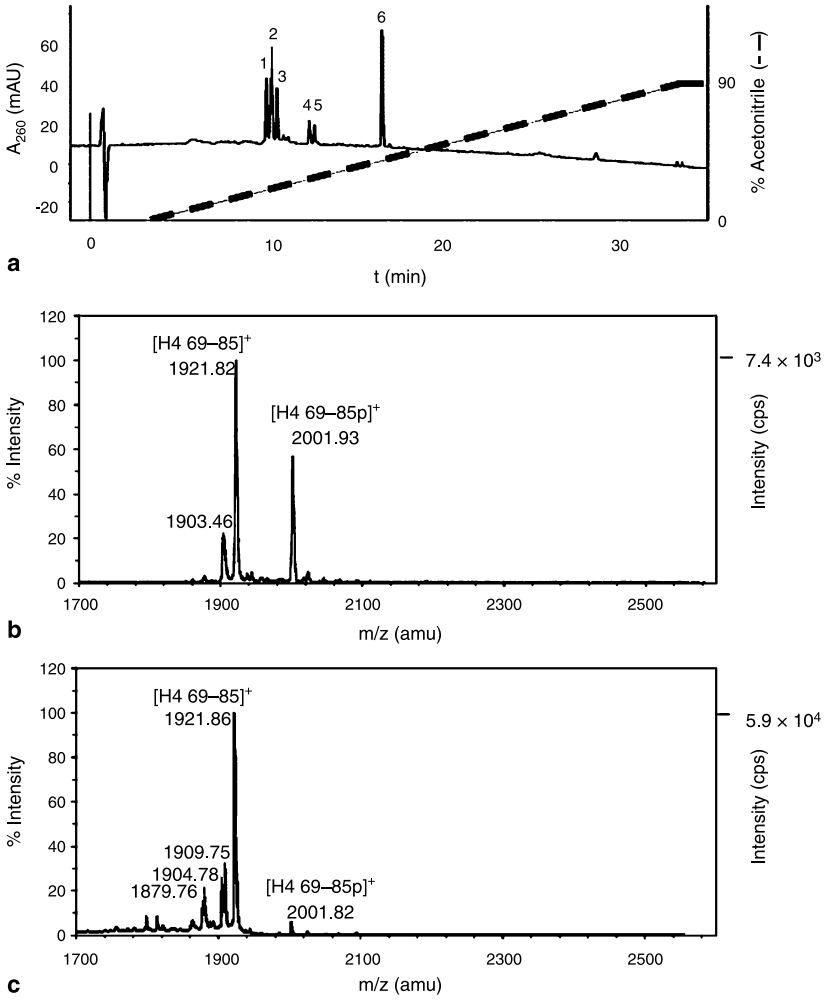

Fig. 5. Reverse-phase HPLC separation of peptides and phosphopeptides in an endoproteinase Asp-N digest of drosphila phosphohistone H4. Chromatogram **a** shows the elution profile of the digest from the reverse-phase column and the acetonitrile gradient. MALDI-TOF-MS analysis of a fraction corresponding to Peak 5 in **a**, in linear mode (**b**), and reflector mode (**c**)

associated with phosphohistidine-containing phosphopeptides, nor is it easy to envisage how a mass-loss of 92 amu could arise.

Reverse-phase HPLC separation of phosphopeptides from the endoproteinase Asp-N digest of drosophila phosphohistone H4

Figure 5a is a chromatogram showing the elution of peptides and phosphopeptides from the reverse phase column. MALDI-TOF-MS analysis was performed on all peak fractions and Fig. 5b and c shows the linear and reflector mode spectra respectively, of a fraction corresponding to Peak 5 in Fig. 5a. The linear spectrum (Fig. 5b) has a major peak with an m/z that closely corresponds to the theoretical m/z (see Table 1) of the phosphopeptide ion $[H4\ 69\text{-}85p]^+$. In addition, there is a peak that corresponds to the theoretical m/z of the peptide ion $[H4\ 69\text{-}85]^+$. The peak at 1903.46 amu in Fig. 5b is suggestive of an ion corresponding to the peptide [H4 69-85] which has lost water (18 amu). In the reflector mode spectrum (Fig. 5c) the ratio of the amplitude of the peak corresponding to $[H4\ 69\text{-}85p]^+$ to that of $[H4\ 69\text{-}85]^+$ has diminished com-

Table 1. Peptides and phosphohistidine-containing phosphopeptides derived from digestion of drosphila histone H4 or phosphohistone H4 with endoproteinase Asp-N, together with the theoretical monoisotopic m/z values of the corresponding singly charged, positive ions

Peptide/ phosphopeptide	Amino acid sequence	m/z (amu)
H4 1-24	MTGRGKGGKGLGKGGAKRHRKVLR	2505.49
H4 1-24p	MTGRGKGGKGLGKGGAKRpHRKVLR	2585.46
H4 2-24	TGRGKGGKGLGKGGAKRHRKVLR	2374.45
H4 2-24p	TGRGKGGKGLGKGGAKRpHRKVLR	2454.42
H4 25-68	DNIQGITKPAIRRLARRGGVKRISGL IYEETRGVLKVFLENVIR	5004.92
H4 69-85	DAVTYTEHAKRKTVTAM	1921.98
H4 69-85p	DAVTYTEpHAKRKTVTAM	2001.95
H4 86-103	DVVYALKRQGRTLYGFGG	2000.07

pared to that in Fig. 5b (0.56–0.07). This is indicative of the occurrence of post-source decay in which the fragmentation of the phosphopeptide, losing HPO_3, is detected. As seen in Fig. 4d, a peak was evident in Fig. 5c (1909.75 amu) that is 92 amu less than the m/z for the phosphopeptide. Again suggestive of an unusual fragmentation of the phosphopeptide associated with phosphohistidine. A peak at 1879.76 amu has also appeared in Fig. 5c, which is 122.06 amu less than the m/z for the phosphopeptide, suggesting another unusual fragmentation of the phosphopeptide. A similar analysis of a fraction corresponding to Peak 4 in Fig. 5a showed only the presence of a peak with an m/z corresponding to [H4 69-85]$^+$. This indicates that good separation of the peptide and phosphopeptide ([H4 69-85] and [H4 69-85p]) has been obtained by reverse-phase HPLC and that much of the [H4 69-85] seen in Peak 5 originates from hydrolysis of [H4 69-85p] between the separation and MALDI-TOF analysis of the fraction.

Analysis of the other peaks in Fig. 5a showed that the major components present were: Peak 1 – [H4 2-24] and [H4 2-24p]; Peak 2 – [H4 1-24] and [H4 1-24p]; Peak 3 – [H4 1-24]; Peak 6 – [86-103]. The good separation of Peaks 3 and 4 is indicative that much of the [H4 1-24] apparent in the analysis of Peak 2 probably derives from hydrolysis of [H4 1-24p], as described above for [H4 69-85p].

ESI-MS analysis of a tryptic digest of phosphohistone H4

Figure 6a shows a precursor ion spectrum for ions with an m/z of −79 amu which is the m/z of the PO_3^-. The two peaks with the highest intensity correspond to precursor ions with m/z values of 390.2 and 606.3 amu. In the MS spectrum shown in Fig. 6b, there appears to be a singly charged ion with a monoisotopic m/z of 390.1285 amu (see Inset (i)) which is close to the theoretical m/z of the singly charged ion of the predicted tryptic phosphopeptide that contains H18 i.e. [H4 18-19p]$^-$ (390.1296 amu). In Inset (ii) there is a doubly charged ion with a monoisotopic m/z of 605.7625 amu which is close to the theoretical m/z of the doubly charged ion of the predicted tryptic phosphopeptide that contains H75 i.e. [H4 68-77p]$^{2-}$ (605.7472 amu). The other major precursor ion observed in Fig. 6a with an m/z of 489.3 amu, appears to correspond to a doubly charged ion in the MS spectrum with a monoisotopic m/z of 489.2208 amu. This does not correspond to any expected tryptic phosphopeptide derived from histone H4, even taking into account possible missed cleavages by the protease and maybe due to a product ion

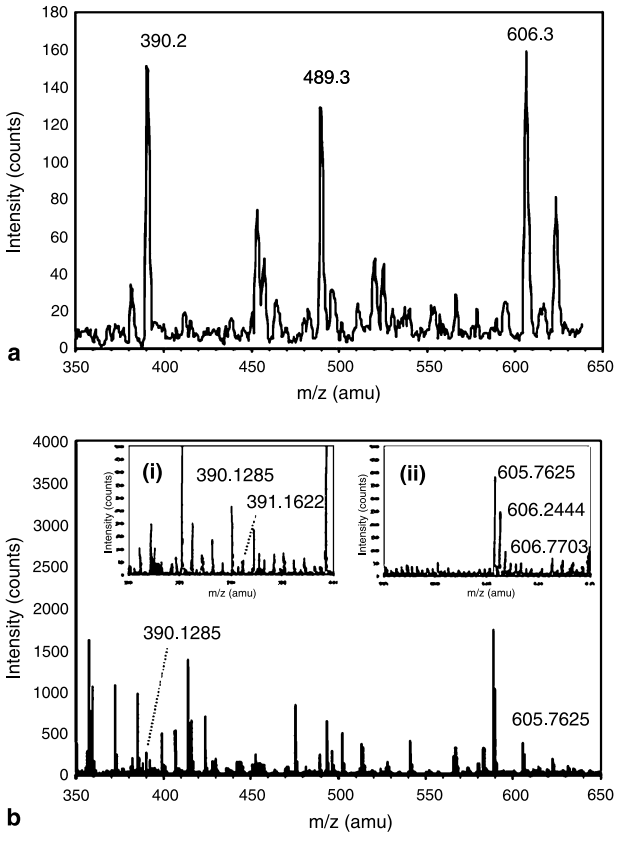

Fig. 6. Negative ion ESI-MS experiments on the tryptic digest of phosphohistone H4. The sample was infused at 5 µl min^{-1} using a declustering potential of −50 V. **a** Precursor ion spectrum detecting the precursors of the −79 amu ion (PO_3^-). 120 scans were accumulated with a collision energy of −50 V. **b** MS scan of the digest where 300 scans were accumulated. Inset (i) is an expanded region of the spectrum from 380 to 400 amu to illustrate the signals that may correspond to the precursor ion seen in **a** at 390.2 amu. Inset (ii) is an expanded region of the spectrum from 595 to 615 amu to illustrate the signals that may correspond to the precursor ion seen in **a** at 605.3 amu

with an m/z of −79 from the fragmentation of an unphosphorylated peptide.

Figure 6b shows the negative ion MS spectrum of the tryptic digest with Insets (i) and (ii) showing expanded regions of the spectrum around the m/z values of the precursor ions observed in Fig. 6a. Inset (i) shows that there are signals corresponding to a singly charged ion with a monisotopic m/z of 390.1285 amu, which is close to that expected for the [H4 18-19p]$^-$ ion. Inset (ii) shows that there are signals corresponding to a doubly charged ion with a monoisotopic m/z value of 605.7625 amu which is close to that expected for the [H4 68-77p]$^{2-}$ ion.

Figure 7 shows the positive ion MS spectrum of a tryptic digest of bovine phosphohistone H4. Inset (i) shows there are signals corresponding to a singly charged ion with a monoisotopic m/z of 392.1822 amu, which is close

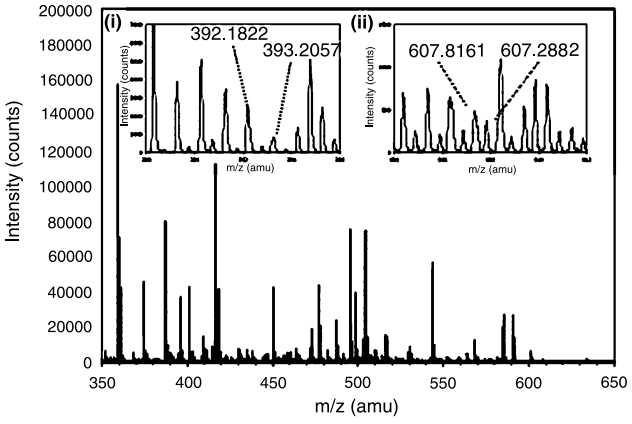

Fig. 7. Positive ion ESI-MS spectrum of tryptic digest of bovine phosphohistone H4. The sample was infused at 2 µl min^{-1} and 150 scans were accumulated. The declustering potential was +20 V. Inset (i) is an expanded region of the spectrum from 388 to 396 amu to illustrate the signals that may correspond to the singly positively charged tryptic phosphopeptide ion $[pHR + H]^+$ (theoretical monoisotopic m/z for this negatively charged ion, $[H4\ 18\text{-}19p]^+ = 392.1441$ amu). Inset (ii) is an expanded region of the spectrum from 604 to 612 amu to illustrate the signals that may correspond to the doubly positively charged tryptic phosphopeptide ion: $[DAVTYTpHAK + 2H]^{2+}$ (theoretical monoisotopic m/z for this negatively charged ion, $[H4\ 68\text{-}77p]^{2+} = 607.7508$ amu)

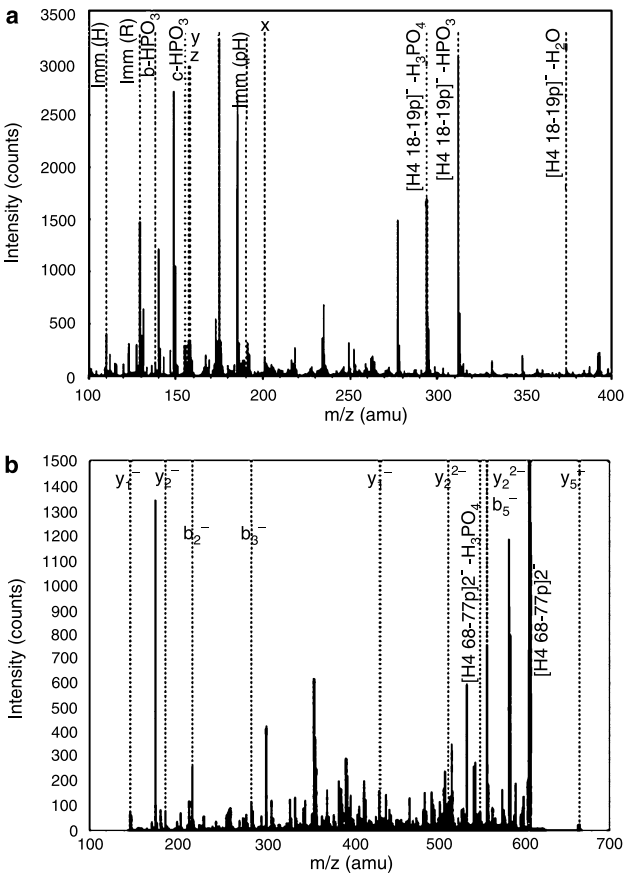

Fig. 8. **a** Positive ion ESI-MS/MS spectrum showing product ions of the possible phosphorylated peptide ion (m/z = 392.1822 amu) ($[pHR + H]^+$, $[H4\ 18\text{-}19p]^+$, m/z = 392.1441 amu) derived from the tryptic digest of bovine phosphohistone H4. A product ion spectrum was obtained where the sample was infused at flow rate of 2 µl min^{-1} with a declustering potential of 20 V and collision energy of 30 V. Vertical dashed lines indicate where the observed signal was within 0.06 amu of the theoretical product ion mass and had minimum peak height equal to 20 counts. These vertical lines are labelled with the corresponding product ion. **b** Positive ion ESI-MS/MS spectrum showing the y and b series product ions of the possible phosphorylated peptide ion (m/z = 607.8271 amu) ($[DAVTYTEpHAK + 2H]^{2+}$, $[H4\ 68\text{-}77p]^{2+}$, m/z = 607.7508 amu) derived from the tryptic digest of bovine phosphohistone H4. A product ion spectrum was obtained where the sample was infused at flow rate of 2 µl min^{-1} with a declustering potential of 20 V and collision energy of 30 V. Vertical dashed lines indicate where the observed signal was within 0.06 amu of the theoretical product y- or b-ion mass and had minimum peak height equal to 20 counts. These vertical lines are labelled with the corresponding product ion

to that expected for the $[H4\ 18\text{-}19p]^+$ ion. Inset (ii) shows there are signals that may correspond to a doubly charged ion with a monoisotopic m/z of 607.8271 amu, which is close to that expected for the $[H4\ 68\text{-}77p]^{2+}$ ion. In this instance, however, the signals are not as clear as in Inset (i) since the signal observed at 607.8271 amu could also be part of an isotopic series of another doubly charged ion with a monoisotopic m/z of 607.3442 amu. In addition, the isotopic series at higher m/z values is obscured by a large signal at 608.4200 amu, although, as indicated in Inset (ii), there is a shoulder on this peak at 608.2882 amu which could correspond to the next isotopic series signal of a doubly charged monoisotopic ion at 607.3442 amu.

In order to confirm that the ions in detected in the positive ion MS spectrum of the tryptic digest of bovine phosphohistone H4 described above, do in fact correspond to the predicted tryptic phosphopeptides pHR ([H4 18-19p]) and DAVTYTEpHAK ([H4 68-77p], product ion experiments were performed. Figure 8a shows the products of collision-induced dissociation of the singly charged ion (∼392 amu) seen in Fig. 7. The vertical dashed lines indicate the positions of signals in the spectrum that match the theoretical m/z values of the expected products of $[H4\ 18\text{-}19p]^+$ (within the constraints detailed in the figure legend). The theoretical masses of these product ions are given in Table 2. Signals corresponding to immonium ions of both histidine and arginine were detected, and most significantly, one corresponding to the immonium ion of phosphohistidine was also detected. Expected x, y and z ions were detected, along with b and c ions, but only the dephospho- forms of these ions. The dehydro- form of the phosphopeptide ion was detected, along with ions corresponding to losses of HPO_3 and H_3PO_4 from the phosphopeptide ion. Taken together, these data provide good evidence that the ion observed in the

Table 2. Product ions of the possible phosphorylated peptide ion (m/z = 392.1822 amu) ($[pHR + H]^+$, $[H4\ 18\text{-}19p]^+$, m/z = 392.1441 amu) derived from the tryptic digest of bovine phosphohistone H4 that correspond to predicted product ions

Product ion	Mass (amu)
Immonium (pHis)	190.0376
Immonium (His)	110.0713
Immonium (Arg)	129.1135
b – HPO_3	138.0662
c – HPO_3	155.0927
x	201.0982
y	175.1190
y – H_2O	157.1084
z	158.0924
$[H4\ 18\text{-}19p]^+$ – H_2O	374.1336
$[H4\ 18\text{-}19p]^+$ – HPO_3	312.2070
$[H4\ 18\text{-}19p]^+$ – H_3PO_4	294.1673

Table 3. Product ions of the possible phosphorylated peptide ion (m/z = 607.8271 amu) ($[DAVTYTEpHAK + 2H]^{2+}$, $[H4\ 68\text{-}77p]^{2+}$, m/z = 607.7508 amu) derived from the tryptic digest of bovine phosphohistone H4 that correspond to predicted product ions

Type of ion	Specific ions detected (charge)
$[H4\ 68\text{-}77p]^{2+}$ – H_3PO_4	(2+)
$[H4\ 68\text{-}77p]^{2+}$ – $(NH_3 + HPO_3)$	(2+)
x – HPO_3	x_3 (1+)
y	y_{1-3}, y_5 (1+); y_{8-9} (2+)
y – NH_3	y_2 (1+); y_6 (2+)
y – HPO_3	y_{1-5} (1+); y_7, y_9 (2+)
y – H_3PO_4	y_{3-6} (1+); y_8 (2+)
y – $(HPO_3 + NH_3)$	y_{2-3}, y_5 (1+); y_8 (2+)
a	a_3 (1+); a_6 (2+)
a – NH_3	a_7 (2+)
b	b_{2-3}, b_5 (1+)
b – H_2O	b_{4-6} (1+)
b – NH_3	b_5 (1+); b_7 (2+)
b – OH	b_{4-5} (1+); b_7 (2+)
c	c_2, c_6 (1+); c_7 (2+)
c – HPO_3	c_9 (2+)

A product ion spectrum was performed where the sample was infused at flow rate of 2 μl min^{-1} with a declustering potential of 20 V and collision energy of 20 V. Matches were positive if the observed signal was within 0.06 amu of the theoretical mass (shown in the table above) and had minimum peak height equal to 20 counts

precursor ion spectrum in Fig. 6a, the negative ion MS spectrum in Fig. 6b and the positive ion MS spectrum in Fig. 7 with monisotopic masses of about 391.1 amu correspond to the tryptic phophopeptide pHR ([H4 18-19p]).

Figure 8b shows the products of collision-induced dissociation of the singly charged ion (~607 amu) seen in Fig. 7. The vertical dashed lines indicate the positions of signals in the spectrum that match the theoretical m/z values of expected y-ion and b-ion products of $[H4\ 68\text{-}77p]^{2+}$ (within the constraints detailed in the figure legend). These and other products of $[H4\ 68\text{-}77p]^{2+}$, where there is a corresponding signal in the product ion spectrum, are given in Table 4. Ions corresponding to the loss of H_3PO_4 and both HPO_3 and NH_3 from the phosphopeptide were detected. In general, there was good coverage of the expected product ions, providing good evidence that the ion observed in the precursor ion spectrum in Fig. 6a, the negative ion MS spectrum in Fig. 6b and the positive ion MS spectrum in Fig. 7 with monoisotopic masses of about 1213.5 amu correspond to the tryptic phophopeptide DAVTYTEpHAK ([H4 68-77p]).

There was good coverage of the y ion series, with six of nine detected, four of these were phosphorylated y ions (out of a possible seven). Two deamino- ($-NH_3$) y ions were detected, but of these only one was phosphorylated. Five out of seven dephospho- ($-HPO_3$) y ions and four out of seven dephospho- ($-H_3PO_4$) y ions were detected. Three out of seven dephospho-, deamino- ($-HPO_3$–NH_3) y ions were detected. Thus overall, 24% of the possible phosphorylated y ions were detected whilst 62% of the unphosphorylated forms were detected. The coverage of the y ions and dephospho- y ions is sufficient to confirm the site of phosphorylation of the peptide as H75.

The coverage of the b ion series was less extensive, with three out of nine b ions, two out of nine dehydro- ($-H_2O$) b ions and two out of nine deamino- ($-NH_3$) and dehydroxy- ($-OH$) b ions were detected (26% overall). Of all of these b ions, none are phosphorylated. In addition, no phosphorylated c ions were detected while 44% of the unphosphorylated forms were, and from Table 3, it can be seen that the phosphorylated b and c ions from $[H4\ 18\text{-}19p]^+$ were also not detected while the unphosphorylated forms were. The lower percentages of phosphorylated product ions detected compared to the unphosphorylated product ions, indicates the instability of the phosphohistidine under these conditions, such that collision-induced dissociation that fragments the peptide chain also tends to remove the phosphoryl group from phosphohistidine.

In the ESI-MS/MS experiments on both the $[H4\ 18\text{-}19p]^+$ and $[H4\ 68\text{-}77p]^{2+}$, no ions corresponding to a mass loss of 92 (or 46 and 92 for $[H4\ 68\text{-}77p]^{2+}$) were observed. Thus the process that seemed to be occurring in the post-source decay MALDI-TOF MS experiments on phosphopeptides in the endoproteinase Asp-N digest of phosphohistone H4 does not seems to occur with the tryptic phosphopeptides in ESI-MS/MS experiments.

We have demonstrated that phosphohistidine in histone H4 that has been phosphorylated on its histidine residues

is sufficiently stable that it can be detected, following overnight pronase E digestion of the phosphoprotein, by ESI-MS and ESI-MS/MS analyses of the digest. Not only can the phosphohistidine be detected in negative ion mode, under very basic conditions where it is stable, it can also be detected under less basic conditions in positive ion mode. It is very useful to be able to perform phosphoamino acid analysis of phosphoproteins by mass spectrometric methods because of their high sensitivity and the obviation of the need to use radiolabelling. In addition, incomplete hydrolysis by pronase E can sometimes lead to unclear phosphoamino acid analyses using conventional ^{32}P-labelling and thin layer chromatography/electrophoresis. A big advantage of a mass spectrometric approach which employs both positive and negative ion MS/MS methods is the greater degree of certainty of identification of phosphohistidine.

We have also shown that phosphopeptides derived from proteolytic digestion of phosphohistone H4, using both trypsin and endoproteinase Asp-N, can also be detected and analysed by mass spectrometry. We have shown that the higher molecular weight phosphopeptides obtained from the endoproteinase Asp-N digests are stable enough to be analysed in MALDI-TOF MS experiments. They can be identified by comparing linear and reflector mode MALDI-TOF MS experiments where post-source decay of the phosphopeptides is observed, leading to loss of the phosphopeptide ion signal. Apart from a mass loss of 80 amu, corresponding to loss of HPO_3 from the phosphopeptides, an unidentified mass loss of 92 amu also appears to be associated with this process. A corresponding mass loss was not observed in the ESI-MS/MS experiments on the tryptic phosphopeptide ions, suggesting that it is particularly associated with a post-source decay process and not collision-induced dissociation in ESI-MS/MS. We have also demonstrated that the phosphopeptides in the endoproteinase Asp-N digests can be separated by reverse-phase HPLC. This suggests that on-line, reverse-phase liquid chromatographic ESI-MS/MS analysis of digests of phosphoproteins containing phosphohistidine will be possible.

We have identified tryptic phosphopeptides by a combination of negative ion precursor scanning for the loss of PO_3^-, negative ion MS, positive ion MS and MS/MS. In the case of phosphodipeptide (pHR) the presence of the immonium ion of phosphohistidine confirms the phosphorylation site. In the case of the phosphodecapeptide (DAVTYTEpHAK), the y ion series detected were comprehensive enough to again confirm the site of phosphorylation of the peptide.

In this work we have shown that if care is taken to employ conditions under which phosphohistidine is reasonably stable, then MS methods that have been employed to study the more well known forms protein phosphorylation, involving phosphoserine, phosphothreonine and phosphotyrosine can also be employed to study protein histidine phosphorylation. We hope that this will lead to a greater understanding of the role of this form of phosphorylation in biological processes.

Acknowledgments

This work was supported by a University of Western Australia Small Grant to P.V.A., a grant from the Raine Medical Research Foundation to P.G.B. and an EMBO Short Term Fellowship to X.L.Z.

References

Besant PG, Attwood PV (2000) Detection of a mammalian histone H4 kinase that has yeast histidine kinase-like enzymic activity. Int J Biochem Cell Biol 32: 243–253

Besant PG, Attwood PV (2005) Mammalian histidine kinases. Biochim Biophys Acta 1754: 281–290

Besant PG, Lasker MV, Bui CD, Turck CW (2000) Phosphohistidine analysis using reversed-phase thin-layer chromatography. Anal Biochem 282: 149–153

Besant PG, Tan E, Attwood PV (2003) Mammalian protein histidine kinases. Int J Biochem Cell Biol 35: 297–309

Bonaldi T, Regula JT, Imhof A (2004) The use of mass spectrometry for the analysis of histone modifications. Methods Enzymol 77: 111–130

Chen CC, Smith DL, Bruegger BB, Halpern RM, Smith RA (1974) Occurrence and distribution of acid-labile histone phosphates in regenerating rat liver. Biochemistry 13: 3785–3789

Chen CC, Bruegger BB, Kern CW, Lin YC, Halpern RM, Smith RA (1977) Phosphorylation of nuclear proteins in rat regenerating liver. Biochemistry 16: 4852–4855

Cuello F, Schulze RA, Heemeyer F, Meyer HE, Lutz S, Jakobs KH, Niroomand F, Wieland T (2003) Activation of heterotrimeric g proteins by a high energy phosphate transfer via nucleoside diphosphate kinase (NDPK) B and Gβ subunits. Complex formation of NDPK B with Gβγ dimers and phosphorylation of His-266 in Gβ. J Biol Chem 278: 7220–7226

Fujitaki JM, Fung G, Oh EY, Smith RA (1981) Characterization of chemical and enzymatic acid-labile phosphorylation of histone H4 using phosphorus-31 nuclear magnetic resonance. Biochemistry 20: 3658–3664

Hippe HJ, Lutz S, Cuello F, Knorr K, Vogt A, Jakobs KH, Wieland T, Niroomand F (2003) Activation of heterotrimeric g proteins by a high energy phosphate transfer via nucleoside diphosphate kinase (NDPK) B and Gβsubunits. Specific activation of Gsα by an NDPK B. Gβγ complex in H10 cells. J Biol Chem 278: 7227–7233

Huang JM, Wei YF, Kim YH, Osterberg L, Matthews HR (1991) Purification of a protein histidine kinase from the yeast *Saccharomyces cerevisiae*. The first member of this class of protein kinases. J Biol Chem 266: 9023–9031

Kikkawa S, Takahashi K, Shimada N, Ui M, Kimura N, Katada T (1990) Conversion of GDP into GTP by nucleoside diphosphate kinase on the gtp-binding proteins. J Biol Chem 265: 21536–21540

Kimura N, Shimada N (1988) Direct interaction between membrane-associated nucleoside diphosphate kinase and GTP-binding protein

(Gs), and its regulation by hormones and guanine nucleotides. Biochem Biophys Res Commun 151: 248–256

Medzihradszky KF, Phillipps NJ, Senderowicz L, Wang P, Turck CW (1997) Synthesis and characterization of histidine-phosphorylated peptides. Protein Sci 6: 1405–1411

Muimo R, Banner SJ, Marshall LJ, Mehta A (1998) Nucleoside diphosphate kinase and Cl^--sensitive protein phosphorylation in apical membranes from ovine airway epithelium. Am J Respir Cell Mol Biol 18: 270–278

Muimo R, Hornickova Z, Riemen CE, Gerke V, Matthews H, Mehta A (2000) Histidine phosphorylation of annexin I in airway epithelia. J Biol Chem 275: 36632–36636

Munoz-Dorado J, Almaula N, Inouye S, Inouye M (1993) Autophosphorylation of nucleoside diphosphate kinase from myxococcus xanthus. J Bacteriol 175: 1176–1181

Napper S, Kindrachuk J, Olson DJ, Ambrose SJ, Dereniwsky C, Ross AR (2003) Selective extraction and characterization of a histidine-phosphorylated peptide using immobilized copper(II) ion affinity chromatography and matrix-assisted laser desorption/ionization time-of-flight mass spectrometry. Anal Chem 75: 1741–1747

Smith DL, Bruegger BB, Halpern RM, Smith RA (1973) New histone kinases in nuclei of rat tissues. Nature 246: 103–104

Stock AM, Robinson VL, Goudreau PN (2000) Two-component signal transduction. Annu Rev Biochem 69: 183–215

Tan E, Zu XL, Yeoh GC, Besant PG, Attwood PV (2003) Detection of histidine kinases via a filter-based assay and reverse-phase thin-layer chromatographic phosphoamino acid analysis. Anal Biochem 323: 122–126

Tan E, Besant PG, Zu XL, Turck CW, Bogoyevitch MA, Lim SG, Attwood PV, Yeoh GC (2004) Histone H4 histidine kinase displays the expression pattern of a liver oncodevelopmental marker. Carcinogenesis 25: 2083–2088

Treharne KJ, Marshall LJ, Mehta A (1994) A novel chloride-dependent GTP-utilizing protein kinase in plasma membranes from human respiratory epithelium. Am J Physiol 267: L592–L601

Treharne KJ, Riemen CE, Marshall LJ, Muimo R, Mehta A (2001) Nucleoside diphosphate kinase – a component of the $[Na^+]$- and $[Cl^-]$-sensitive phosphorylation cascade in human and murine airway epithelium. Pflugers Arch 443 [Suppl 1]: S97–S102

Uesaka H, Yokoyama M, Ohtsuki K (1987) Physiological correlation between nucleoside-diphosphate kinase and the enzyme-associated guanine nucleotide binding proteins. Biochem Biophys Res Commun 143: 552–559

Wei YF, Matthews HR (1990) A filter-based protein kinase assay selective for alkali-stable protein phosphorylation and suitable for acid-labile protein phosphorylation. Anal Biochem 190: 188–192

Wei YF, Matthews HR (1991) Identification of phosphohistidine in proteins and purification of protein-histidine kinases. Methods Enzymol 200: 388–414

Wind M, Wegener A, Kellner R, Lehmann WD (2005) Analysis of CheA histidine phosphorylation and its influence on protein stability by high-resolution element and electrospray mass spectrometry. Anal Chem 77: 1957–1962

Authors' address: Paul V. Attwood, School of Biomedical, Biomolecular and Chemical Sciences (M310), The University of Western Australia, 35 Stirling Highway, Crawley, WA 6009, Australia,
Fax: +61 8 6488 1148, E-mail: pattwood@cyllene.uwa.edu.au